3B.3   OBSERVATIONS AND QUANTIFICATION OF COUNTER-ROTATING MESOVORTEX COUPLETS WITHIN THE 8 MAY 2009 SOUTHERN MISSOURI DERECHO

Angela D. Lese*
NOAA/National Weather Service, Louisville, Kentucky

Steven Martinaitis
OU/CIMMS - NOAA/NWS Warning Decision Training Branch, Norman, Oklahoma

1. INTRODUCTION

There have been ample observational and numerical studies conducted on bow echoes and squall lines, especially since the Bow Echo and MCV Experiment (BAMEX; Davis et al. 2004). These quasi-linear convective systems (QLCSs) are well-known producers of damaging straight-line winds. Many studies have shown that the descending rear-inflow jet (RIJ) at the bow echo apex can be responsible for damaging surface winds (Fujita 1978; Przybylinski 1995). Additional research has shown that damaging winds at the surface can be attributed to leading-line circulations, or mesovortices (e.g., Funk et al. 1999; Arnott and Atkins 2002; Trapp and Weisman 2003). This is especially true when mesovortices are located just north of the RIJ apex.   Enhancement of the ground-relative winds on the southern periphery of the mesovortex have been shown to produce a concentrated swath of extreme straight-line wind damage (Atkins et al. 2005; Wakimoto et al. 2006; Wheatley et al. 2006).   Furthermore, mesovortices have also been shown to be the parent circulations of squall line and bow echo tornadoes (e.g., Funk et al. 1999; Atkins et al. 2004, 2005).   Bow echo tornadoes typically produce EF0-EF2 wind damage at the surface (Atkins and St. Laurent 2009a), but they are capable of producing EF3-EF4 tornado wind damage as well (Trapp et al. 2005).

Whatever the resultant damage within a QLCS, the most intense damage can be attributed to mesovortices.   The rapid development and dissipation of mesovortices in conjunction with their shallow vertical profile can often create a difficult warning environment for operational forecasters. These challenges have led to recent numerical studies focused on the genesis mechanism of QLCS mesovortices (e.g., Trapp and Weisman 2003; Wakimoto et al. 2006; Atkins and St. Laurent 2009b). In all of these simulations, counter-rotating (cyclonic and anticyclonic) mesovortex pairs were identified; however, cyclonic mesovortices without a companion anticyclonic mesovortex are predominantly documented in observational studies.   The only known case of observed counter-rotating vortex couplets within a QLCS structure was in the 6 July 2003 bow echo via dual-Doppler airborne data (Wakimoto et al. 2006). From this event, Wakimoto et al. (2006) and Wheatley and Trapp (2008) attributed the vortex couplet genesis to tilting cold-pool vortex lines via mechanically generated downdrafts, which resulted in the anticyclonic vortex forming to the north of the cyclonic vortex. A quasi-idealized simulation of the 6 July 2003 bow echo was also conducted by Atkins and St. Laurent (2009b).   The results of this numerical study showed vortex couplets with the cyclonic vortex forming to the north by the upward tilting of cold-pool generated vortex lines from a localized updraft maximum.   The discrepancy in the genesis mechanism is not well understood, and thus, finding a conceptual model for mesovortex genesis remains challenging without observational consistency.
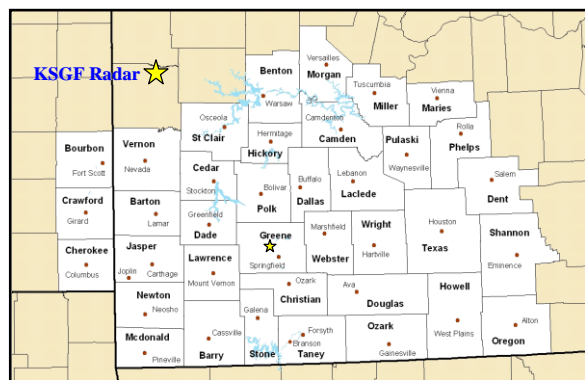

Fig. 1. Map of the SGF CWA. County names (bold black) and county seats are shown above.

---

*Corresponding author address: Angela Lese, National Weather Service
6201 Theiler Lane, Louisville, KY 40229-1476
e-mail: Angela.Lese@noaa.gov

The 8 May 2009 derecho may have provided this consistency, as well as the first observed counter-rotating mesovortex pair(s) within a QLCS structure as seen from a surface-based Doppler radar. These suggested pair(s) may also be the first observed vortex couplets where the cyclonic mesovortex formed to the north of the anticyclonic mesovortex. An observational analysis has been performed here on this particular event, where an intense QLCS moved through the County Warning Area (CWA) of the National Weather Service (NWS) Weather Forecast Office (WFO) in Springfield, Missouri (SGF; Fig. 1) during the morning hours of 8 May 2009. This study will examine the two possible counter-rotating mesovortex couplets in detail using single-Doppler radar data. These findings and their implications to the operational warning environment will also be discussed.

2. SYNOPTIC AND MESOSCALE OVERVIEW

The synoptic environment in place that morning was that of a typical warm-season pattern for bow echoes described in Johns and Hirt (1987). This is represented by weak dynamics producing mid-level ridging or northwesterly flow, low-level warm and moist advection near the bow-echo initiation area, and a weak instability boundary usually oriented parallel to the mean wind direction, along which the bow-echo typically advances. Initial convection formed in a region of isentropic upglide in northeast Colorado within the right-entrance region of a 30-35 m s^{-1} 500 hPa jet around 0400 UTC 8 May 2009. Above average precipitable water content enhanced by strong moisture return associated with a 25 m s^{-1} 850 hPa low-level jet aided in the development and progression of a QLCS through southern Kansas and into southern Missouri.

The maturation of the QLCS and the development of an unusually large and intense northern bookend vortex occurred over the SGF CWA. The 1200 UTC sounding from SGF (not shown) was very unstable with most unstable convective available potential energy (MUCAPE) around 4000 J kg^{-1} with strong 0-3 km storm relative helicity of over 250 m^2 s^{-2}. The combination of the strong environmental shear and the descending RIJ allowed for rapid formation of mesovortices and provided an enhanced tornadic potential with the QLCS. NWS storm survey teams from SGF determined that 19 tornadoes occurred in the SGF CWA, as well as large swaths of straight-line wind damage from 35-40 m s^{-1} winds.

3. OBSERVATIONS ANALYSIS ON COUNTER-ROTATING VORTEX COUPLETS

Over 30 user-identified mesovortices can be classified using the SGF WSR-88D reflectivity and velocity data. The majority of these were cyclonic. Only two of the cyclonic mesovortices were associated with an anticyclonic mesovortex.

a. Brighton mesovortex couplet analysis

The first possible counter-rotating mesovortex couplet was observed at 1316 UTC near the town of Brighton, MO. The couplet will hereafter be denoted as the Brighton mesovortex couplet. Radar reflectivity and single-Doppler storm-relative velocity data from the SGF WSR-88D of the Brighton mesovortex couplet evolution are shown in Fig. 2. Also plotted on each reflectivity image is the position of the gust front based on spectrum width analysis. Both mesovortices were first identified at 1316 UTC and coexisted through the 1330 UTC volume scan. The vortex couplet was located to the north of the WSR-88D at a range of 20 km at 1316 UTC to a range of 38 km at 1330 UTC. General motion of the cyclonic (anticyclonic) vortex was from 203° at 24.7 m s^{-1} (218° at 22.6 m s^{-1}). The cyclonic and anticyclonic vortices diverged from each other at a rate of 8 m s^{-1} after genesis.

The cyclonic (anticyclonic) vortex originated from the northern (southern) extent of a 40 m s^{-1} outbound velocity maximum along the gust front, as shown in the base velocity data (Fig. 3). The gust front is locally accelerated between the two mesovortices, as seen in the gust front analysis and radar reflectivity in Figs. 2a and 2b, with the location of each mesovortex collocated with a perturbation of the gust front. The bulge created in the gust front becomes less pronounced at 1325 and 1330 UTC (Figs. 2c and 2d) as the wind maxima became associated with the diverging vortices.

Time-height diagrams of rotational velocity (V_r) for both mesovortices are shown in Fig. 4. A NWS storm survey confirmed an EF1 tornado developed with the cyclonic vortex at 1316 UTC approximately 3.1 km northwest of Brighton, MO. The tornado lasted for ten minutes and
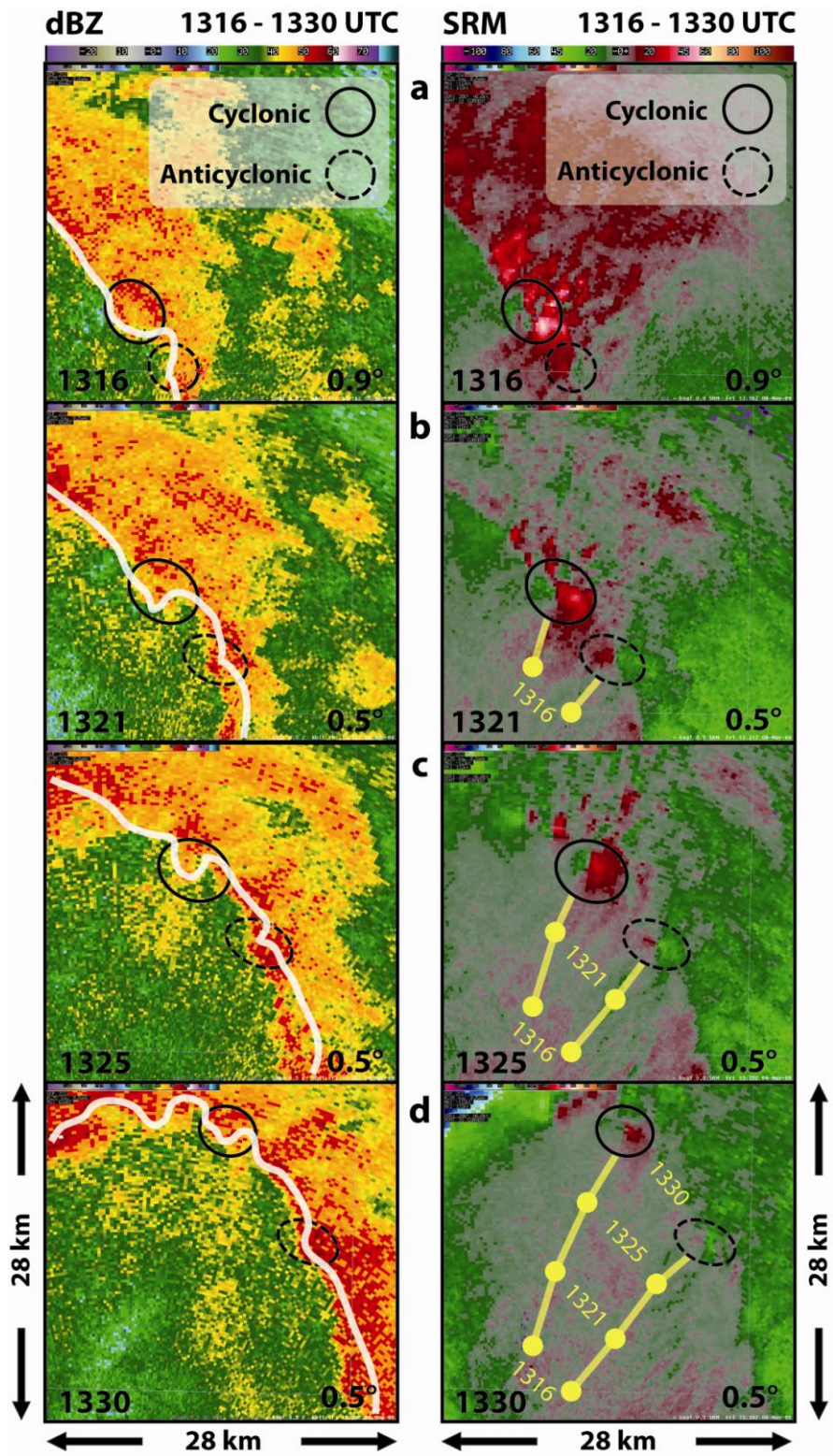
Fig. 2. Radar reflectivity (dBZ) and single-Doppler storm relative motion velocity (SRM) from the SGF WSR-88D at (a) 1316, (b) 1321, (c) 1325, and (d) 1330 UTC. The SGF WSR-88D is located south of the couplet at a range of 20 km (a) to 38 km (d). The solid (dashed) black oval highlights the location of the cyclonic (anticyclonic) mesovortex. The white line represents the position of the gust front based on spectrum width analysis. The solid yellow lines represent the path of each mesovortex with the previous positions denoted by solid yellow points and time (in UTC).
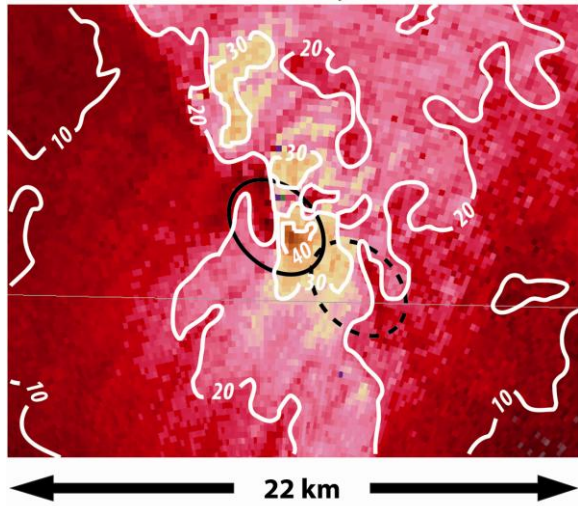
V - 0.5° Tilt   **8 May 2009 - 1316 UTC**

← **22 km** →

Fig. 3. Single-Doppler base velocity (V) data from the 0.5° tilt of the SGF WSR-88D at 1316 UTC. The white contours are of V in 10 m s^{-1} intervals. The solid (dashed) black oval highlights the location of the cyclonic (anticyclonic) mesovortex.
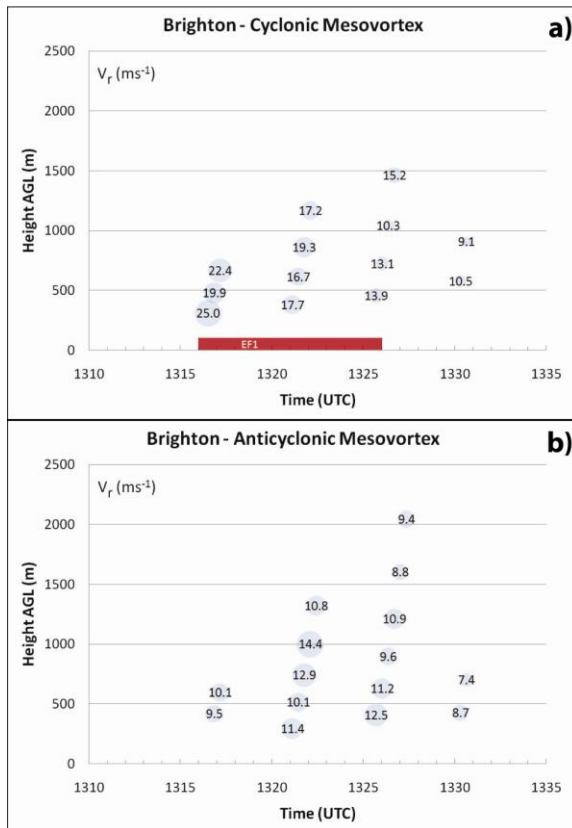

Fig. 4. Time-height profiles of V_r (m s^{-1}) for the (a) cyclonic and (b) anticyclonic mesovortex. The intensity and times of tornado damage are shown by the red bar along the horizontal axis.

produced a damage path length of 13.9 km at a maximum width of 229 m. The non-tornadic anticyclonic mesovortex is remarkably weaker than the cyclonic mesovortex, with an average V_r difference of 11 m s^{-1} (5 m s^{-1}) over comparable velocity data at 1316 UTC (1321 UTC). Note that the anticyclonic vortex is non-distinguishable at the 0.5° tilt at 1316 UTC. The anticyclonic vortex extends higher into the vertical than the cyclonic vortex at both 1321 and 1325 UTC. The reason for this is currently not understood, but this may be due to sampling limitations between radar volumetric scans.

b. Bradleyville mesovortex couplet analysis

The second possible counter-rotating mesovortex couplet was observed at 1325 UTC near the town of Bradleyville, MO. This couplet will hereafter be denoted as the Bradleyville mesovortex couplet. The evolution of the Bradleyville mesovortex couplet has notably significant differences when compared to the Brighton mesovortex couplet. Radar reflectivity and single-Doppler storm-relative velocity data from the SGF WSR-88D of the mesovortex couplet evolution from 1325 to 1339 UTC are shown in Fig. 5. Also plotted on each reflectivity image is the position of the gust front based on spectrum width analysis. The vortex couplet was located to the south-southeast of the WSR-88D at an average range of 55 km from 1330 to 1339 UTC. General motion of the cyclonic (anticyclonic) vortex was from 231° at 28.3 m s^{-1} (244° at 24.2 m s^{-1}). The cyclonic and anticyclonic vortices diverged from each other at a rate of 9 m s^{-1} after genesis of the anticyclonic mesovortex.

The cyclonic mesovortex can be identified as early as 1321 UTC, nine minutes before anticyclonic mesovortex development. This differs from the synchronous development of the cyclonic/anticyclonic vortices of the Brighton vortex couplet. It was noted that the Bradleyville anticyclonic mesovortex did not form along the gust front. It was also noted that a pronounced secondary boundary, as denoted in Fig. 5a, existed at 1325 UTC in the spectrum width product (Fig. 6). This feature became less identifiable in time due to a significant area of enhanced spectrum width values in the region (not shown). It can be hypothesized that the anticyclonic mesovortex formed along this secondary boundary. A strong non-tornadic cyclonic mesovortex is located approximately 8
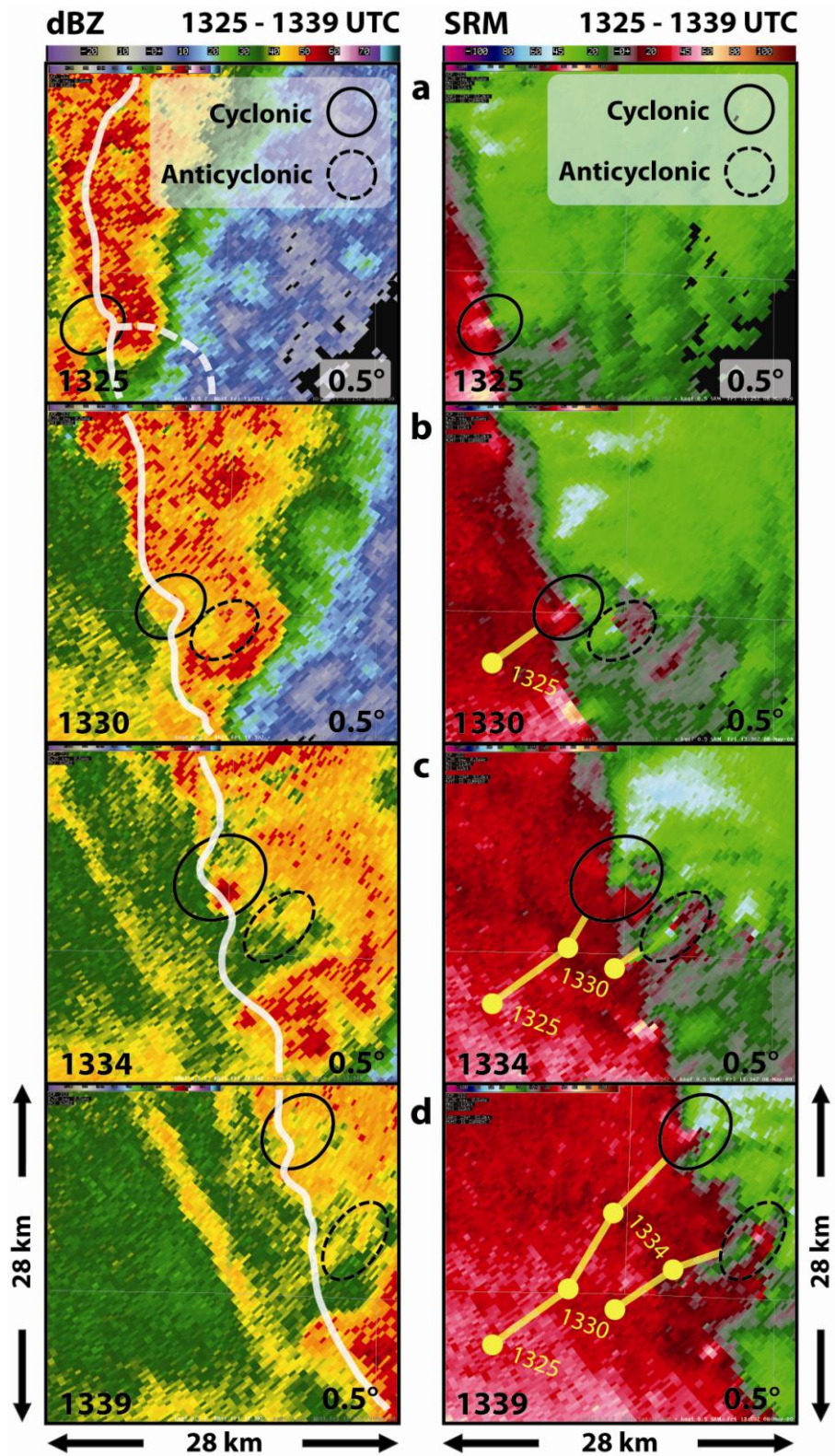
Fig. 5. Same as Fig. 2 except for the Bradleyville mesovortex couplet at (a) 1325, (b) 1330, (c) 1334, and (d) 1339 UTC. The SGF WSR-88D is located northwest of the couplet at a range of approximately 55 km (a-d). The dashed white line in (a) represents the position of a secondary boundary based on spectrum width analysis.
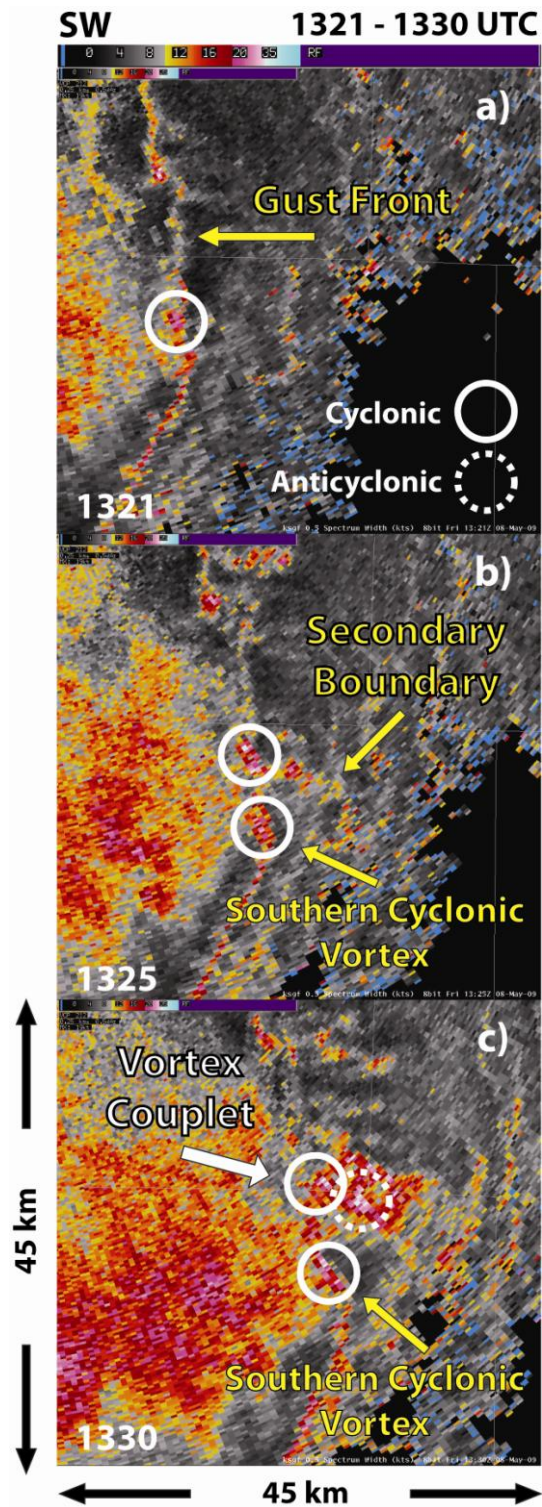
Fig. 6. Spectrum width values from the SGF WSR-88D from (a) 1321, (b) 1325, and (c) 1330 UTC. The solid (dashed) white circles highlight the location of all cyclonic (anticyclonic) mesovortices. The gust front is identified in (a), and the secondary boundary is identified in (b). The white arrow in (c) denotes the location of the Bradleyville mesovortex couplet.
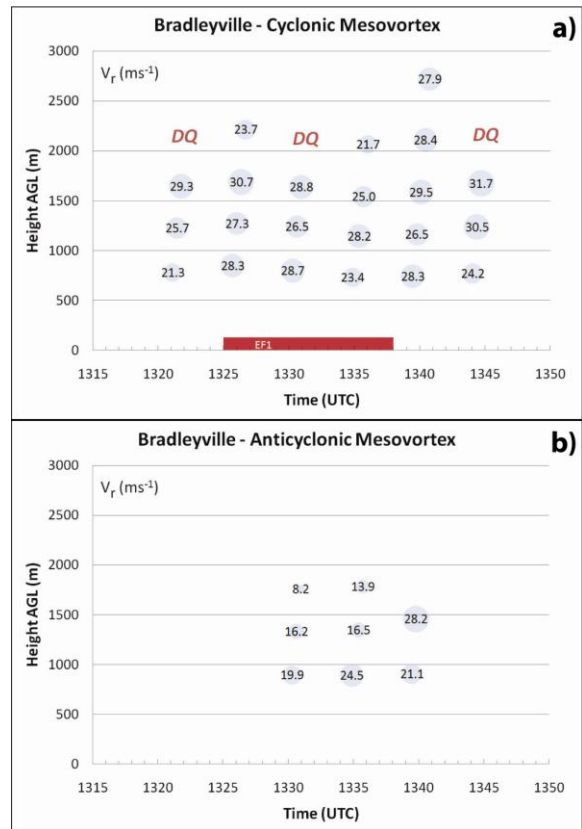

Fig. 7. Same as Fig. 4 except for the Bradleyville mesovortex couplet. Profiles with data quality issues are denoted with a red DQ.

km to the south of the vortex couplet from 1325 UTC to 1334 UTC. It is not understood whether this cyclonic vortex or the secondary boundary influenced the Bradleyville vortex couplet.

Time-height diagrams of V_r for both mesovortices are shown in Fig. 7. A NWS storm survey confirmed an EF1 tornado developed with the cyclonic vortex at 1325 UTC approximately 4.5 km southeast of Swan, MO. The tornado lasted for 13 minutes and produced a damage path length of 19.7 km at a maximum width of 805 m. Data quality issues with the velocity data prevented proper analysis of the cyclonic mesovortex, which are denoted in Fig. 7a. Similar to the Brighton mesovortex couplet, the cyclonic vortex is stronger than the anticyclonic vortex during the existence of the vortex couplet. One unusual observation regarding the anticyclonic vortex was the overall increase in V_r from 1330 to 1339 UTC before an abrupt dissipation between the 1339 and 1344 UTC WSR-88D volume scans (Fig. 7b). In contrast, the cyclonic mesovortex of the

Bradleyville vortex couplet had a greater vertical extent than the anticyclonic vortex, even with the aforementioned data quality issues. Both vortices were also stronger than these associated with the Brighton vortex couplet. This could be a result of their proximity to the descending RIJ apex.

4. IMPLICATIONS ON OPERATIONS

The characteristics of both mesovortex couplets were carefully analyzed in order to determine their validity and their effect on warning operations. The authors realize that suggesting these counter-rotating mesovortex couplets are the first ones ever documented by surface-based Doppler radar reflectivity and velocity data within a QLCS is presumptuous given the lack of data supporting this claim. However, their existence and evolution is consistent with the Atkins and St. Laurent (2009b) conceptual model on cyclonic-anticyclonic mesovortices. Furthermore, NWS operational forecasters use single-Doppler radar reflectivity and velocity data nearly exclusively to issue severe thunderstorm and tornado warnings. Thus, the authors assume that the findings in this study are sufficient to claim that counter-rotating mesovortex couplets may have potential implications on operations and NWS warnings.

The mesovortices that formed during the 8 May 2009 event are consistent with previous findings in that they can be quite transient, forming and dissipating quickly and often times without advanced notice (e.g., Wolf 2000; Atkins et al. 2004; Wheatley et al. 2006). Thus, it can be said with confidence that mesovortex-dominant QLCS events provide an extremely difficult warning environment for operational forecasters. Furthermore, sampling issues from single-Doppler radar data add an element of difficulty. If the WSR-88D is sampling a transient mesovortex or one far from the radar location, significant changes to the vortex may occur in between radar volumetric scans and vertical slices. Additionally, the radar beam width increases as it travels further from the radar, making it more difficult to resolve mesovortices (on the order of ~10 km). Lastly, this situation becomes even more challenging with the addition of counter-rotating mesovortex couplets for several possible reasons.

First, both cyclonic vortices produced an EF1 tornado in the 8 May 2009 event. It is unknown whether it is common for the cyclonic component of a vortex couplet in a QLCS to become tornadic due to lack of observational examples. It is also unknown whether or not to discount the anticyclonic component as being non-tornadic because of the lack of examples. What can be speculated, however, is that an anticyclonic mesovortex may produce enhanced straight-line wind damage. Documentation of any future observations and analysis regarding counter-rotating mesovortex couplets is necessary, as well as conducting highly detailed damage surveys, even if damage was not reported. Conducting an increased number of diligent damage surveys is a foreseeable workload or staffing challenge that NWS personnel will have to overcome in order to build statistics on what type of damage, if any, each mesovortex produces.

Second, the cyclonic and anticyclonic vortices in both vortex couplets had divergent motion. The movement of cyclonic mesovortices tends to be left of system-scale motion. Having short-lived counter-rotating mesovortices diverging from each other could result in difficultly creating the correct warning polygon orientation, encompassing the correct path and threat area from each component. In the case of the Brighton mesovortex couplet, the cyclonic member was tornadic when first detected by the WSR-88D at 1316 UTC (Fig. 4a). Thus, it would have required an immediate tornado warning upon detection. The complexity of warning on rapidly developing, divergent mesovortices is further compounded by having to determine the general motion and threat area from only one or two WSR-88D volumetric scans.

Finally, general NWS warning methodology for a QLCS is to issue larger, storm-based severe thunderstorm warning polygons that encompass the wind threat associated with bowing line segments and bookend vortices. Upgraded warnings can be issued for strong mesovortices if they are considered to be or reported to be tornadic. Non-tornadic mesovortices have been shown to produce intense straight-line damaging near-surface winds. The locally accelerated gust front between the cyclonic and anticyclonic vortices can also create enhanced straight-line wind damage. Enhanced wording describing the

increased straight-line wind damage threat for a defined region should be used in severe weather statements that update severe thunderstorm warnings.

5. SUMMARY

The 8 May 2009 derecho was an extreme QLCS with numerous tornadic and non-tornadic mesovortices and perhaps the first documented counter-rotating mesovortex couplets as seen from surface-based single-Doppler radar data in a QLCS. The Brighton mesovortex couplet is closest to the SGF WSR-88D and provides more confidence to the authors' claim, whereas the Bradleyville couplet, given its increased distance from the radar and data quality issues, is more difficult to confirm.

Under the claim that these are, in fact, counter-rotating mesovortex couplets, both cyclonic members showed stronger V_r values, with each cyclonic mesovortex producing an EF-1 tornado. It was also found that the cyclonic (anticyclonic) member of the vortex pair was oriented to the north (south), which is similar to the vortex couplet orientation presented by Atkins and St. Laurent (2009b); however, the details of the vortex couplet genesis are not understood. Future work will include the use of high spatial and temporal resolution analysis from the Local Analysis and Prediction System (LAPS) software which will add support to this case and will hopefully shed light on the mesovortex-genesis matter.

6. REFERENCES

Arnott, J. M., and N. T. Atkins, 2002: Tornadogenesis within quasi-linear convective systems. Part 1: Radar and storm damage analysis of the 29 June 1998 derecho. Preprints, *21st Conf. on Severe Local Storms*, San Antonio, TX, Amer. Meteor. Soc., 494-497.

Atkins, N. T., J. M. Arnott, R. W. Przybylinski, R. A. Wolf, and B. D. Ketcham, 2004: Vortex structure and evolution within bow echoes. Part 1: Single-Doppler and damage analysis of the 29 June 1998 derecho. *Mon. Wea. Rev.*, **132**, 2224-2242.

_____, N. T., C. S. Bouchard, R. W. Przybylinski, R. J. Trapp, and G. Schmocker, 2005: Damaging surface wind mechanisms within the 10 June 2003 Saint Louis bow echo during BAMEX. *Mon. Wea. Rev.*, **133**, 2275-2296.

_____, and M. St. Laurent, 2009a: Bow echo mesovortices. Part I: Processes that influence their damaging potential. *Mon. Wea. Rev.*, **137**, 1497-1513.

_____, and M. St. Laurent, 2009b: Bow echo mesovortices. Part II: Their genesis. *Mon. Wea. Rev.*, **137**, 1514-1532.

Davis, C., and Coauthors, 2004: The bow-echo and MCV experiment (BAMEX): Observations and opportunities. *Bull. Amer. Meteor. Soc.*, **85**, 1075-1093.

Fujita, T. T., 1978: Manual of downburst identification for project Nimrod. Satellite and Mesometeorology Research Paper 156, Dept. of Geophysical Sciences, University of Chicago, 104 pp.

Funk, T. W., K. E. Darmofal, J. D. Kirkpatrick, V. L. DeWald, R. W. Przybylinski, G. K. Schmocker, and Y.-J. Lin, 1999: Storm reflectivity and mesocyclone evolution associated with the 15 April 1994 squall line over Kentucky and southern Indiana. *Wea. Forecasting*, **14**, 976-993.

Johns, R. H. and W. D. Hirt, 1987: Derechos: Widespread convectively induced wind-storms. *Wea. Forecasting*, **2**, 32-49.

Przybylinski, R. W., 1995: The bow echo: Observations, numerical simulations, and severe weather detection methods. *Wea. Forecasting*, **10**, 203-218.

Trapp, R. J., and M. L. Weisman, 2003: Low-level mesovortices within squall lines and bow echoes. Part 2: Their Genesis and Implications. *Mon. Wea. Rev.*, **131**, 2804-2823.

_____, R. J., S. A. Tessendorf, E.S. Godfrey, and H. E. Brooks, 2005: Tornadoes from squall lines and bow echoes. Part I: Climatological distribution. *Wea. Forecasting*, **20**, 23-34.

Wakimoto, R. M., H. V. Murphey, C. A. Davis, and N. T. Atkins, 2006: High winds generated by bow echoes. Part II: The relationship between the mesovortices and damaging straight-line winds. *Mon. Wea. Rev.*, **134**, 2813-2829.

Wheatley, D. M., R. J. Trapp, and N. T. Atkins, 2006: Radar and damage analysis of severe bow echoes observed during BAMEX. *Mon. Wea. Rev.*, **134**, 791-806.

_____, D. M., and R. J. Trapp, 2008: The effect of mesoscale heterogeneity on the genesis and structure on mesovortices within quasi-linear convective systems. *Mon. Wea. Rev.*, **11**, 4220-4241.

Wolf, R. A., 2000; Characteristics of circulations associated with the 29 June 1998 derecho in eastern Iowa. Preprints, *20th Conf. on Severe Local Storms*, Orlando, FL, Amer. Meteor. Soc., 56-59.